

## NUMERICAL ANALYSIS OF CLOSURE CRITERIA FOR SPECTRAL VISCOELASTIC CONSTITUTIVE EQUATIONS USED IN THE CLASSICAL MELT SPINNING MODEL

Marta B. Peirotti, Mariel L. Ottone and Julio A. Deiber

*Instituto de Desarrollo Tecnológico para la Industria Química  
(INTEC-UNL-CONICET)*

*Güemes 3450, S3000GLN, Santa Fe, Argentina*

*e-mail: [treoflu@santafe-conicet.gov.ar](mailto:treoflu@santafe-conicet.gov.ar)*

**Key words:** Melt Spinning Flow, Finite Differences, Spectral Viscoelastic Models, Elongational Flow

**Abstract.** The classical melt spinning model is reformulated to include a spectral rheological constitutive equation for an arbitrary number of modes composing the spectra of relaxation times and modules. This resulting spectral spinning model requires a closure criterion to be applied in the iteration of the spinning initial condition of the total stress tensor, at the onset of the stretching zone. Thus this stress value must be distributed, at each one of the iterations, among the stress modes of the spectral viscoelastic rheological model, the sum of which shall be consistent with the total stress value. For this purpose different closure criteria are generated in the literature to carry out this stress distribution. Without loss of generality, in this work we study numerically this particular problem for the isothermal condition only. A new closure criterion is proposed and analyzed in relation to previous ones. In general it is found that two zones are clearly distinguished along the stretching flow: one, where numerical results of the process elongational viscosity are insensitive to the closure criterion used, and the other involving the counterpart situation.

## 1 INTRODUCTION

The melt spinning operation is used in the polymer processing industry to produce textile fibers. In this operation the polymer melt is subject to a complex non isothermal and predominantly extensional flow. Computational models providing axial velocity, stress and temperature profiles are still under study. One reason explaining this situation is that, in applications, different viscoelastic constitutive models must be considered depending on the type of material to be processed, generating thus several numerical complexities. In this context of analysis, the classical and most used melt spinning model, in the low take up velocity range, has been widely analyzed and also revised in the literature, mainly for viscoelastic rheological models with one relaxation time only (see, for instance, Denn, 1980, and Ottone and Deiber, 2002). In practice, however, one needs usually a spectrum of relaxation times to describe appropriately the rheometric functions of a given polymer melt through the constitutive equation selected, which may frequently require from two to ten stress modes and relaxation times (Bernnat, 2001). Thus, for any spectrum size, one common numerical problem appears when the classical melt spinning model includes a spectral rheological model. This problem is associated with the closure criterion to be applied in the iteration of the spinning initial condition of the total stress tensor, at the onset of the stretching zone. Thus this stress value must be distributed at each one of the iterations among the  $M$  stress modes of the spectral viscoelastic rheological model, the sum of which shall be consistent with the total stress value. For this purpose different closure criteria are generated in the literature to carry out this stress distribution starting from the last  $M$  mode to the first one (see Gagon and Denn, 1981 and Devereux and Denn, 1994, for the case of two stress modes and relaxation times). Without loss of generality, in this work we study numerically this particular problem for the isothermal condition only, through our previous algorithm for spinning flow (Ottone and Deiber, 2002) now adapted for spectral viscoelastic rheological models, where different closure criteria must be imposed, and hence studied here. It is found that two zones are clearly distinguished along the stretching flow: one, where numerical results are insensitive to the closure criterion used, and the other involving the counterpart situation.

Numerical results of the process elongational viscosity as a function of the rate of elongation are also discussed within the map of the true elongational and shear viscosities for three different closure criteria, indicating the physical characteristics of the spinning flow in relation to these two relevant non linear rheometric curves. The basic melt spinning model is reformulated in general for the spectral  $M$  modes of stresses, within the framework of our previous computational algorithm based on finite differences to obtain, the axial velocity profile and the thermal and stress fields in the 2-D domain of the filament. In this sense, it should be observed here that this domain reduces systematically to a 1-D domain under the isothermal condition considered in this work. To achieve our purpose here, after a coordinate transformation to get a rectangular numerical domain, the perturbation analysis of the full spinning model reported by Henson et al. (1998) was applied again by including specifically the spectra of stress modes and relaxation times. Thus this model was formulated for the low speed range (flow induced crystallization was not considered) through a regular perturbation analysis (see details in Section 4 below) that included the slenderness approximation associated with long fibers of very small diameters. Here the Phan-Thien and Tanner viscoelastic constitutive equation with an arbitrary number of stress modes and relaxation times, appropriate to describe extensional and shear flows simultaneously, is used to illustrate our conclusions for the isothermal spinning flow.

The numerical study is carried out for a branched low density polyethylene (LDPE9) melt rheologically characterized here through the Phan-Thien and Tanner spectral viscoelastic constitutive equation with experimental data reported by Bernnat (2001).

## 2 THE SPECTRAL TENSORIAL PHAN-THIEN AND TANNER MODEL

The spectral Phan-Thien and Tanner model (PTTM) for the total stress tensor  $\underline{\underline{\tau}} = \underline{\underline{\tau}}_p + \underline{\underline{\tau}}_s$  is decomposed into the spectral polymer contribution,  $\underline{\underline{\tau}}_p = \sum_{m=1}^M \underline{\underline{\tau}}_m$ , and the term associated with retardation effects,  $\underline{\underline{\tau}}_s = 2\eta_s \underline{\underline{D}}$  (Peirotti et al., 2006). In this sense, one expresses,

$$\underline{\underline{\tau}}_m + \lambda_m^e \frac{\delta}{\delta t} \underline{\underline{\tau}}_m = 2\lambda_m^e G_m \underline{\underline{D}} \quad m = 1, \dots, M \quad (1)$$

where  $\lambda_m^e$  is the effective relaxation time (see below), and

$$\frac{\delta}{\delta t} \underline{\underline{\tau}}_m = \frac{D}{Dt} \underline{\underline{\tau}}_m - \underline{\underline{L}} \cdot \underline{\underline{\tau}}_m - \underline{\underline{\tau}}_m \cdot \underline{\underline{L}}^T \quad m = 1, \dots, M \quad (2)$$

is the non affine convective time derivative (Ottone et al., 2006) adapted here for isothermal spinning. Also  $\underline{\underline{L}} = \nabla \underline{\underline{v}} - \chi \underline{\underline{D}}$  is the effective velocity gradient tensor. Further,  $\underline{\underline{v}}$  is the velocity vector,  $\underline{\underline{D}}$  is the rate of deformation tensor and  $\chi$  is the chain slip parameter. We

define  $\eta_s = \eta_p(1 - \alpha)/\alpha$  and  $\eta_p = \sum_{m=1}^M \lambda_m^e G_m$ , hence, the instantaneous elastic response of this model may be obtained for  $\alpha = 1$  (Denn, 1990). Consistently, the zero shear rate viscosity of the melt is expressed  $\eta_o = \eta_p + \eta_s$ . In particular, the PTTM considers effective relaxation times  $\lambda_m^e = \lambda_m / K_m (tr \underline{\underline{\tau}}_m)$  that are functions of the trace invariant of the stress tensor and  $K_m = \exp[\xi tr \underline{\underline{\tau}}_m / G_m]$ . Also  $\{\lambda_m\}$  and  $\{G_m\}$  are the spectra of relaxation times and modules, respectively, as obtained from the linear viscoelastic response.

The constitutive model expressed through Eqs. (1) and (2) allows one to determine the spectra of relaxation times and modules  $\{\lambda_m, G_m\}$  with experimental data of the storage  $G'$  and loss  $G''$  modules as functions of frequency  $\omega$ , which are obtained from Bernnat (2001).

These rheometric functions in terms of the spectra of relaxation times and modules are,

$$G'(\omega) = \sum_{m=1}^M G_m \frac{\lambda_m^2 \omega^2}{(1 + \lambda_m^2 \omega^2)} \quad (3)$$

$$G''(\omega) = \sum_{m=1}^M G_m \frac{\lambda_m \omega}{(1 + \lambda_m^2 \omega^2)} \quad (4)$$

The algorithm used to fit experimental data is composed of two parts. One involves a linear least squares procedure with linear inequality constraints imposing that  $\{\lambda_m\}$  must be a positive value for physical meaning (see, for example, Deiber et al., 1997; Peirotti et al., 1998). The other part of the algorithm uses a nonlinear regression analysis through the Levenberg-Marquardt subroutine to minimize the fitting error on the average, thus providing an improved final set  $\{\lambda_m, G_m\}$ . Despite that fitting procedures cannot provide a unique set

$\{\lambda_m, G_m\}$ , which is a well known limitation in numerical calculations fully described elsewhere, results obtained in this work for the spectra of relaxation times and modules of LDPE9 are quite similar to those reported by Bernnat (2001).

Therefore in order to determine the remaining non linear rheological parameters, Eqs. (1) and (2) are written in the cylindrical coordinate system for both the shear and elongational flows to fit experimental data reported by Bernnat (2001) for these test kinematics (see Peirotti et al., 2006, for further details).

Thus, Eqs. (1) and (2) in shear flow yield,

$$\frac{\partial \tau_m^{zz}}{\partial t} = -\frac{K_m}{\lambda_m} \tau_m^{zz} + \tau_m^{rz} \dot{\gamma} \left(1 - \frac{\chi}{2}\right) + \tau_m^{zr} \dot{\gamma} \left(1 - \frac{\chi}{2}\right) \quad m = 1, \dots, M \quad (5)$$

$$\frac{\partial \tau_m^{rr}}{\partial t} = -\frac{K_m}{\lambda_m} \tau_m^{rr} - \tau_m^{rz} \dot{\gamma} \frac{\chi}{2} - \tau_m^{zr} \dot{\gamma} \frac{\chi}{2} \quad m = 1, \dots, M \quad (6)$$

$$\frac{\partial \tau_m^{zr}}{\partial t} = -\frac{K_m}{\lambda_m} \tau_m^{zr} + \tau_m^{rr} \dot{\gamma} \left(1 - \frac{\chi}{2}\right) - \tau_m^{zz} \dot{\gamma} \frac{\chi}{2} + G_m \dot{\gamma} \quad m = 1, \dots, M \quad (7)$$

$$\frac{\partial \tau_m^{\theta\theta}}{\partial t} = -\frac{K_m}{\lambda_m} \tau_m^{\theta\theta} \quad m = 1, \dots, M \quad (8)$$

$$K_m = \exp \left[ \frac{\xi}{G_m} (\tau_m^{zz} + \tau_m^{rr} + \tau_m^{\theta\theta}) \right] \quad m = 1, \dots, M \quad (9)$$

where,

$$\underline{\underline{D}} = \begin{pmatrix} 0 & \frac{1}{2} \dot{\gamma} & 0 \\ \frac{1}{2} \dot{\gamma} & 0 & 0 \\ 0 & 0 & 0 \end{pmatrix} \quad (10)$$

and  $\dot{\gamma} = dv_z / dr$  being the shear rate. In addition,  $\tau_s^{zz} = \tau_s^{rr} = \tau_s^{\theta\theta} = 0$  and  $\tau_s^{zr} = \eta_s \dot{\gamma}$ .

A procedure to find the shear stress  $\tau = \tau^{zr} = \sum_{m=1}^M \tau_m^{zr} + \tau_s^{zr}$  and the shear viscosity function

$\eta = \tau / \dot{\gamma}$  is to solve these equations numerically from the inception of the shear flow until the asymptotic steady state is reached. In order to calculate this steady state, the time derivatives in Eqs. (5) to (8) are written in discrete form. Then the Runge-Kutta method is applied until stresses are constant. The time step used in this work is  $10^{-5}$  s. Criteria for convergence at the steady state are expressed in terms of two consecutive time steps, as follows,

$$\left| \left( \sum_{m=1}^M \tau_m^{pq} \right)^{i+1} - \left( \sum_{m=1}^M \tau_m^{pq} \right)^i \right| / \left| \left( \sum_{m=1}^M \tau_m^{pq} \right)^i \right| \leq 10^{-6} \quad (11)$$

where superscripts  $p$  and  $q$  refer to cylindrical coordinates (see Eqs. (5) to (9)) and  $i$  indicates the number of time steps being carried out.

For the purpose of quantifying the stresses of the melt LDPE9 under rheometric elongational flow, we solved Eqs. (1) and (2) for,

$$\underline{\underline{D}} = \begin{Bmatrix} \dot{\epsilon} & 0 & 0 \\ 0 & -\frac{1}{2}\dot{\epsilon} & 0 \\ 0 & 0 & -\frac{1}{2}\dot{\epsilon} \end{Bmatrix} \quad (12)$$

where  $\dot{\epsilon}$  is the elongational rate, and in this case,  $\tau_m^{rr} = \tau_m^{\theta\theta}$ . In a similar situation as the one described above for the shear rate rheometry, steady stresses cannot be obtained explicitly in elongational flow from the rheological model and the kinematics expressed by Eq. (12).

Therefore, the elongational viscosity  $\eta_e = (\sum_{m=1}^M \tau_m^{zz} - \sum_{m=1}^M \tau_m^{rr}) / \dot{\epsilon}$ , is found here by solving numerically the following equations for the inception of the elongational flow toward the asymptotic steady state,

$$\frac{\partial \tau_m^{zz}}{\partial t} = -\frac{K_m}{\lambda_m} \tau_m^{zz} + 2\tau_m^{zz} (1 - \chi) \dot{\epsilon} + 2G_m \dot{\epsilon} \quad m = 1, \dots, M \quad (13)$$

$$\frac{\partial \tau_m^{rr}}{\partial t} = -\frac{K_m}{\lambda_m} \tau_m^{rr} - \tau_m^{rr} (1 - \chi) \dot{\epsilon} - G_m \dot{\epsilon} \quad m = 1, \dots, M \quad (14)$$

$$\frac{\partial \tau_m^{\theta\theta}}{\partial t} = -\frac{K_m}{\lambda_m} \tau_m^{\theta\theta} - \tau_m^{\theta\theta} (1 - \chi) \dot{\epsilon} - G_m \dot{\epsilon} \quad m = 1, \dots, M \quad (15)$$

$$K_m = \exp \left[ \frac{\xi}{G_m} (\tau_m^{zz} + 2\tau_m^{rr}) \right] \quad m = 1, \dots, M \quad (16)$$

Once more, in order to calculate normal stresses, we write the time derivatives in Eqs. (13) to (15) in discrete form, and then apply the same numerical procedure as that used for the shear flow analyzed above. Through Eqs. (1) to (16), the spectral PTTM is used to characterize the LDPE9 with data from shear and elongational rheometry reported by Bernnat (2001). Thus, once the spectra of relaxation times and modules  $\{\lambda_m, G_m\}$  and rheological parameters  $\alpha$ ,  $\xi$  and  $\chi$  are determined, this constitutive equation is ready to be used in the isothermal spinning model. Rheological parameters for the LDPE9 characterized with the spectral PTTM are reported in Section 5.

### 3 SPECTRAL ISOTHERMAL SPINNING MODEL

Although, our previous model was reformulated in general to include spectral constitutive equations under non isothermal flow condition, for the present work, we analyze the isothermal spinning flow only, which is simpler enough to illustrate clearly the performance of closure criteria under analysis, as proposed in Section 1 and presented and discussed below. The impact of these criteria on the numerical evaluation of the process elongational viscosity is of course the target of the present research. In addition, the isothermal melt spinning flow has relevance to characterize rheometrically polymer melts in pure elongational flow (see, for instance, Ottone et al., 2006, for a review of relationships proposed in the literature for this purpose).

Therefore, in this section the isothermal melt spinning model for the steady state regime is described briefly through the basic general expressions. Thus, the polymer is considered incompressible and the mass balance implies,

$$(\underline{\nabla} \cdot \underline{v}) = 0 \quad (17)$$

where  $\underline{v}$  is the velocity vector. The balance of momentum in the filament is expressed,

$$\rho \underline{v} \cdot \underline{\nabla} \underline{v} = -\underline{\nabla} p + \underline{\nabla} \cdot \underline{\underline{\tau}} + \rho \underline{g} \quad (18)$$

where  $\rho$  is the polymer density,  $p$  is the pressure field,  $\underline{g}$  is the gravity vector and  $\underline{\underline{\tau}}$  is the stress tensor considered symmetric throughout this work. Further, in the spinning model  $r_o(z)$  is the fiber radius as a function of the axial direction  $z$ ,  $v_s$  is the melt velocity at the beginning of the stretching zone with radius  $r_s$  and after the maximum swelling. Thus,  $v_s = v_c r_c^2 / r_s^2$  where  $v_c$  is the melt averaged velocity in the extrusion capillary of radius  $r_c$ . At the end of the spinneret  $z = z_L = L$ , the take up velocity is  $v_z = v_L$ ; hence the draw ratio is  $DR = v_L / v_s$ .

The appropriate set of boundary conditions to solve Eqs (17) and (18) is taken directly from Denn (1980, 1990). For this purpose the fluid kinematics is  $\underline{v}(r, z) = v_z \underline{e}_z + v_r \underline{e}_r$ , where  $v_z$  and  $v_r$  are the axial and radial components of the velocity vector respectively (see also Section 4), in the cylindrical coordinate system. Initial values for  $\tau_s^{zz}$  and  $\tau_s^{rr}$  are needed at

$z=0$ , apart from the stress  $\tau_p^{zz}$  and the relation  $R = \frac{\tau_p^{rr}}{\tau_p^{zz}}$ , already discussed in the literature

(Ottone and Deiber, 2002). At this position the properties are assumed uniform in the radial direction, which for any value of  $r$  are,

$$v_z(0) = v_s \quad r_o(0) = r_s \quad \tau^{zz}(0) = \tau_o^{zz} \quad (19)$$

Although the stress ratio  $R$  may be varied in the range  $-1/2 < R < 0$  for viscoelastic fluids,  $R \approx 0$  is a good approximation (Denn, 1980 and 1983; Ottone and Deiber, 2002).

It is clear from Eq. (19) that the spectral constitutive equation must distribute the  $M$  different stress modes through appropriate stress relations in order to meet a convergent value of the total stress  $\tau_o^{zz}$ . Consequently a closure criterion for these calculations is required in the iteration process of the spinning initial condition of the total stress tensor, at the onset of the stretching zone. For this purpose different criteria were generated in the literature to carry out this stress distribution starting from the last  $M$  mode to the first one. Thus Gagon and Denn (1981) recommended,

$$\tau_m^{zz} = \tau_o^{zz} \lambda_m / \sum_{m=1}^M \lambda_m \quad (20)$$

while Devereux and Denn (1994) later suggested,

$$\tau_m^{zz} = \tau_o^{zz} \lambda_m^2 G_m / \sum_{m=1}^M \lambda_m^2 G_m \quad (21)$$

In particular we propose here the following expression,

$$\tau_m^{zz} = \tau_o^{zz} \lambda_m G_m / \sum_{m=1}^M \lambda_m G_m \quad (22)$$

Closure criteria expressed through Eqs. (20) and (22) are based on the physical hypothesis that each stress mode participates in the total stress value proportionally to either the fraction of mode relaxation time or the fraction of mode viscosity. The mode fraction used in Eq. (21) is rather hybrid involving, however, the product of mode relaxation time and mode viscosity  $\eta_m = G_m \lambda_m$ . The effects of Eqs. (20) to (22) in the spinning flow solution subject to the constraint  $\tau_m^{rr} / \tau_m^{zz} \approx 0$  at  $z=0$ , with  $m = 1, \dots, M$  are studied and discussed below.

Boundary conditions involving the symmetry of fields are imposed at the centerline  $r = 0$  for any position  $z$ . Thus,

$$\frac{\partial v_z}{\partial r} = 0, \quad \frac{\partial \tau^{zz}}{\partial r} = 0 \quad \frac{\partial \tau^{rr}}{\partial r} = 0 \quad (23)$$

At the filament free surface for  $r = r_o(z)$  and any position  $z$ , dynamics and kinematics constraints are,

$$(\underline{T} \cdot \underline{n}) \cdot \underline{t} = (\underline{T}_a \cdot \underline{n}) \cdot \underline{t} \quad (24)$$

$$(\underline{T} \cdot \underline{n}) \cdot \underline{n} = -\sigma \mathfrak{K} + (\underline{T}_a \cdot \underline{n}) \cdot \underline{n} \quad (25)$$

$$\underline{v} \cdot \underline{n} = 0 \quad (26)$$

$$\underline{v} \cdot \underline{t} = \underline{v}_a \cdot \underline{t} \quad (27)$$

In these equations,  $\underline{n}$  and  $\underline{t}$  are the unit vectors normal and tangential to the free surface, respectively,  $\mathfrak{K}$  is the curvature of the free surface and  $\sigma$  is the polymer-air surface tension. In addition, the complete melt stress tensor  $\underline{T} = -p\underline{\delta} + \underline{\tau}$  involves the extra stress tensor  $\underline{\tau}$  (see Eqs. (1) and (2)) and the pressure  $p$ , where  $\underline{\delta}$  is the unit tensor. Here the complete stress tensor and the velocity of the surrounding air are designated  $\underline{T}_a$  and  $\underline{v}_a$ , respectively. It is important to visualize that in particular for the isothermal spinning flow of this work the air transversal flow is imposed at the same temperature as that of the fiber at the extrusion capillary, so that the isothermal melt condition is kept along the whole spinneret. Therefore, by following Peirotti et al. (2005), here we also define  $\underline{T}_a = -p\underline{\delta} + 2\eta_a \underline{D}_a$ , where  $\eta_a$  is the air viscosity and  $\underline{D}_a$  is the air shear rate tensor, which is a function of  $\underline{v}_a$ . Thus, Eqs. (24) to (27) are relevant for the general formulation of the spinning flow, and they effectively evaluate the isothermal interaction between the spinning fiber and the surrounding air.

From the above equations one concludes that even under isothermal conditions the full spinning model is quite complex to be solved directly. Therefore this model is simplified through a perturbation analysis as described in Section 4, below. Further, in the classical spinning flow, the Newtonian kinematics of the air around the fiber is not solved locally; instead, well consolidated correlations are used to establish the air shear stress in Eq. (24) as explained below.

#### 4 ASPECTS ON THE NUMERICAL SOLUTION OF THE SPINNING MODEL

In this section, the main numerical steps followed to solve the isothermal spinning model described above are presented only. A detailed description of the algorithm used here may be found in Ottone and Deiber (2002) for the more general case of non isothermal spinning flow.

Thus, first a coordinate transformation is carried out by defining a new normalized coordinate  $\zeta = r/r_o(z)$ . Then a regular perturbation analysis is applied to Eqs. (1) and (2) and (17) to (27) according to the scheme proposed by Henson et al. (1998). For this purpose the full model described in Section 3 may be expressed in dimensionless form by using appropriate scales (Henson et al. (1998)). On this base, any dependent variable, represented by  $P$  in the generalized sense, is expressed  $P = \sum_{n=0}^{\infty} \Lambda^n P^{(n)} = P^{(o)} + \mathcal{O}(\Lambda)$ , where  $\Lambda$  is the ratio between the capillary radius and the stretching length of the filament. Consequently, in the regular perturbation analysis, terms of order  $\Lambda$  and greater are neglected to introduce the slenderness hypothesis. This scheme allows one to neglect rigorously terms of small orders from the balance and constitutive equations, and the boundary conditions of the full model, described in Section 3. For instance, the shear stress  $\tau_a^{nt}$  in Eq. (24) is directly reduced to  $\tau_a^{zr}$ , which is evaluated from a correlation involving the friction coefficient and the air velocity  $v_a$  obtained from Eq. (27) (see Ottone and Deiber, 2000 and 2002, for details). Further, it is also shown that  $\tau_a^{nn}$  is of the order of  $\Lambda$  and hence it may be neglected in Eq. (25).

The resulting isothermal model with this procedure is rather simple and the stress field is uniform in the radial direction of the filament. More interesting is the fact that the perturbed model thus obtained is equivalent to the average model described by Ottone and Deiber (2002) for the non isothermal case. Therefore the isothermal model may be expressed in the

matrix form  $\dot{\underline{x}} = \underline{\underline{A}}^{-1}(\underline{x}) \cdot \underline{b}$  where  $\dot{\underline{x}} = \left\{ \frac{\partial v_z}{\partial z}, \frac{\partial f}{\partial z}, \frac{\partial \tau}{\partial z} \right\}$  and  $f = \frac{\partial v_z}{\partial z}$ . Equation  $\dot{\underline{x}} = \underline{\underline{A}}^{-1}(\underline{x}) \cdot \underline{b}$

can be solved with the appropriate initial conditions for velocity and stresses as reported above. Nevertheless, in practice one may estimate the value of the axial velocity  $v_s$  at the initial position of the extrusion process only. Unfortunately, the initial stresses are not known beforehand and they must be found through a numerical iterative process already described in the literature (see, for instance, Papanastasiou et al., 1996). In the framework of cylindrical coordinates  $r$  and  $z$ , the iterative process consists of initializing the viscoelastic tension components  $\tau_p^{zz}$  and  $\tau_p^{rr}$  at  $z = 0$ . This position is placed after the maximum swelling of the filament by taking  $f \approx 10$  (see also a discussion on this aspect in Ottone and Deiber, 2000 and 2002). Then the system of equations described above is solved iteratively with the fourth order Runge-Kutta method, until one reproduces the value assigned to  $v_L$  at  $z=L$ , with the following convergence criterion  $|v_z^k(L) - v_L|/|v_L| \leq 10^{-6}$ , where  $k$  indicates the number of axial step size used to reach  $L$ . Thus a two-point-boundary value problem must be solved. It should be observed that only one total stress (viz.,  $\tau_p^{zz}(0)$  at the initial condition) shall be iterated while the other is fixed with the constant ratio  $R = \tau_p^{rr} / \tau_p^{zz}$ . Further the distribution of mode stresses here must follows one of the closure criteria under analysis in this work.

The numerical code is written in FORTRAN language, and the axial step size is fixed at  $10^{-5}$  m. This value is small enough to achieve appropriately the convergence criterion concerning the take up velocity  $v_L$ . Thus numerical results of rheometric and spinning viscosities are precise enough to test the theories under consideration below.

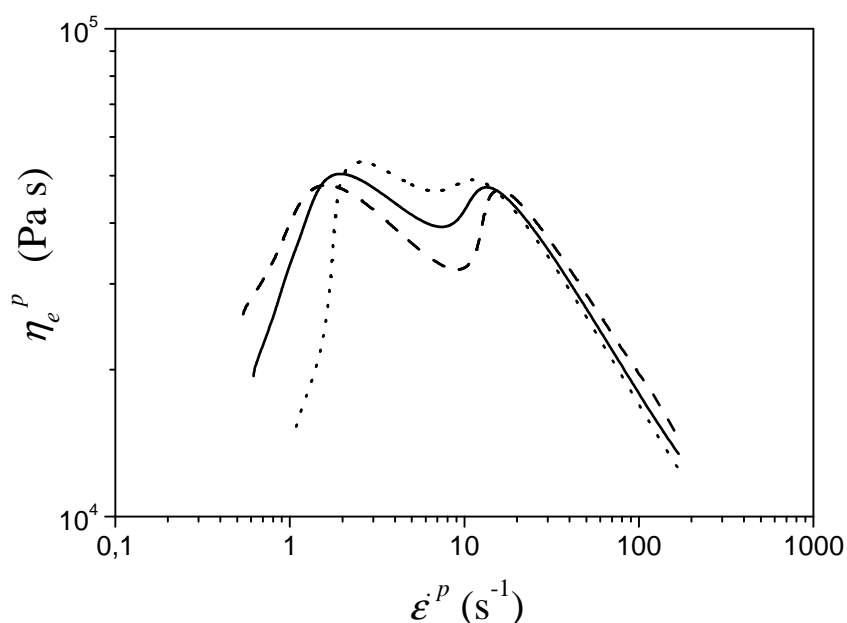
Finally, once the numerical solutions for axial velocity and stress fields are available, one can calculate the process extensional viscosity as follows,

$$\eta_e^p(\dot{\epsilon}^p) = \frac{(\tau^{zz} - \tau^{rr})^p}{\dot{\epsilon}^p} \quad (28)$$

where the process extensional rate is obtained from  $\dot{\epsilon}^p = (\partial v_z / \partial z)^p$  by using the spinning axial velocity. Equation (28) is useful to analyze closure criteria in Section 5. In this equation super index  $p$  indicates “process”.

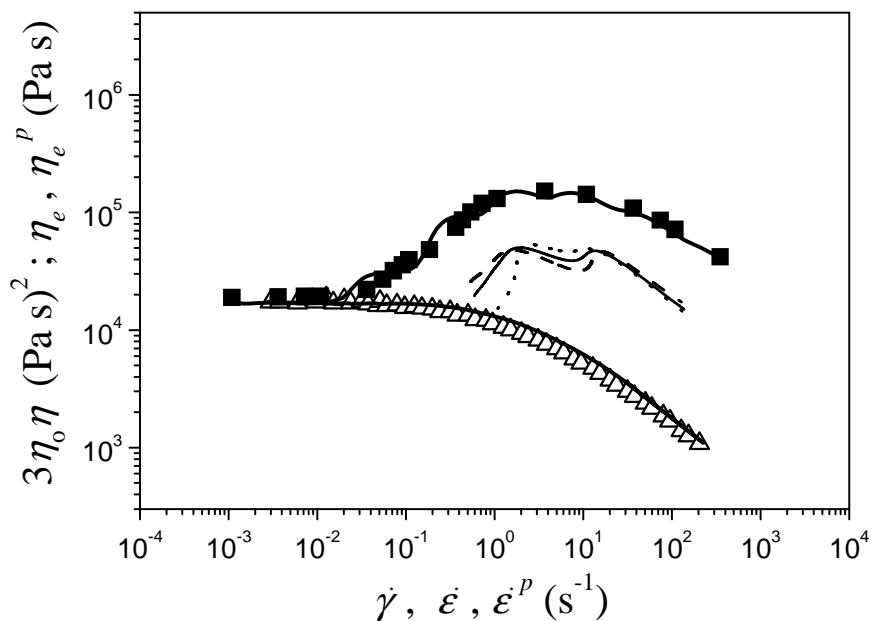
## 5 RESULTS AND DISCUSSION

Figure 1 shows the process elongational viscosity as a function of the process elongational rate for LDPE9 ( $M=7$ ,  $\alpha = 0.99$ ,  $\xi=0.013$ ,  $\chi = 0.1$ ) at  $T = 190$  °C. The three criteria have been considered when  $v_c = 0.012$  m/s,  $v_s = 0.006$  m/s,  $z_L = 10$  cm and  $DR=200$ . In this figure two zones are clearly distinguished along the stretching flow. One is present at high elongational rates where numerical results are rather insensitive to closure criteria, while the other involves the counterpart situation at low elongational rates.



**Figure 1:** Process elongational viscosity as a function of the process elongational rate for LDPE9. Also  $v_c = 0.012$  m/s,  $v_s = 0.006$  m/s,  $z_L = 10$  cm and  $DR=200$ . Lines indicate numerical predictions with different closure criteria: (·····) Eq. (20), (---) Eq. (21) and (—) Eq. (22).

This melt spinning situation may be also observed in Figure 2 where numerical results of the process elongational viscosity for different closure criteria are depicted within the map of the true elongational and shear viscosities. It is found that the values of the process elongational viscosity obtained from the melt spinning model is in between the elongational and shear rheometric viscosity curves in a rather short range of deformation rate. This aspect is relevant mainly to characterize rheometrically polymer melts in pure elongational flow



**Figure 2:** Process elongational viscosity for different closure criteria depicted within the map of the true elongational (upper curve) and shear (lower curve) viscosities. Symbols are rheometric data from Bernnat (2001) for LDPE9, where full lines show the PTM fittings. Also  $v_c = 0.012$  m/s,  $v_s = 0.006$  m/s,  $z_L = 10$  cm and  $DR=200$  are process variable. Other lines indicate numerical predictions of process elongational viscosity for different closure criteria: (·····) Eq. (20), (---) Eq. (21) and (—) Eq. (22).

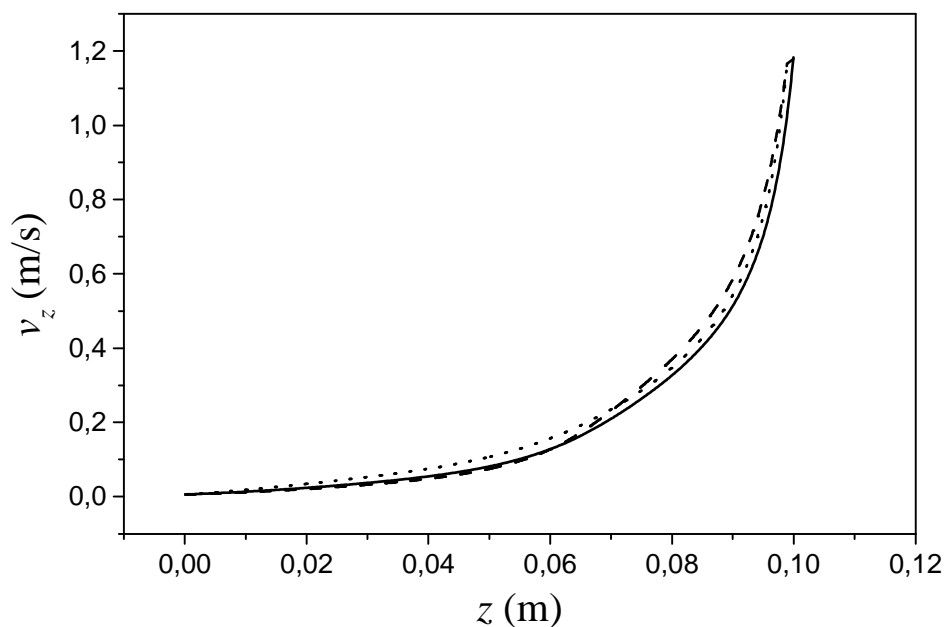


**Figure 3:** Axial velocity profile as a function of the spinneret position for LDPE9. Also  $v_c = 0.012$  m/s,  $v_s = 0.006$  m/s,  $z_L = 10$  cm and  $DR=200$ . Lines indicate numerical predictions with different closure criteria: (·····) Eq. (20), (---) Eq. (21) and (—) Eq. (22).

(Ottone et al., 2006) in the sense that the rheometric and process elongational viscosity curves are numerically different although their shapes may be similar.

Figure 3 shows the prediction of the axial velocity profile through the isothermal spinning model when closure criteria are used for LDPE9. Numerical results indicate that closure criteria provide quite similar velocity profiles for the melt under consideration. On the other hand, small differences on the axial velocity field are reflected in rather important differences of the process elongational viscosity, as illustrated in Figures 1 and 2. Nevertheless, this particular conclusion is not necessarily general and further comparison with experimental data is required. This task is being carried out at the present for other polymer melts and spinning velocity experimental data available in the literature. The presence of wiggles in the curves of rheometric and process elongational viscosities (Figures 1 and 2) is characteristic in results coming from the use of spectral constitutive models. Although one expects they do not have physical meaning, it is clear that there exists a compromised situation between predicting well and simultaneously the apparent and elongational rheometric viscosities against obtaining rather a smooth process elongational viscosity

## 5 CONCLUSIONS

Numerical results from the isothermal melt spinning model shows that the application of different closure criteria at the onset of the spinning flow for the spectral PTTM, generates two zones along the stretching domain: one is present at high elongational rates where numerical results are rather insensitive to closure criteria, while the other involves the counterpart situation at low elongational rates. Also it is found that the values of the process elongational viscosity obtained from the melt spinning model is lower than the rheometric elongational viscosity. This aspect is relevant mainly to characterize rheometrically polymer melts in pure elongational flow. Finally, further numerical studies and comparison with experimental data of the spinning velocity and mainly stresses are required to indicate which criterion is better to assign the spectrum of stresses at the initial condition of the melt spinning flow.

## Acknowledgments

Authors wish to thank the financial aid received from Universidad Nacional del Litoral, Santa Fe, Argentina (CAI+D 2006) and CONICET (PIP 5728).

## REFERENCES

- Bernnat, A. Polymer melt rheology and the rheotens test. Doctoral Thesis, 2001.
- Deiber, J. A., Peirotti, M. B., and Gappa, A. The linear viscoelastic relaxation modulus related to the mwd of linear homopolymer blends. *J. Elast. and Plastics*, 29: 290-313, 1997.
- Denn, M. M. Issues in viscoelastic flow. *Ann. Rev. Fluid Mech.*, 22: 13-32, 1990.
- Denn, M. M. *Computational Analysis of Polymer Processing*. Pearson, J. R. A., Richardson, S. M. Eds.; Applied Science Publishers. New York, 1983.
- Denn, M. M. Continuous drawing of liquids to form fibers. *Ann. Rev. Fluid Mech.*, 12: 365-387, 1980.
- Devereux, B. M., and Denn, M. M. Frequency response analysis of polymer melt spinning. *Ind. Eng. Chem. Res.*, 33: 2384 – 2390, 1994.
- Gagon, D. K., and Denn, M. M. Computer simulation of steady polymer melt spinning. *Polym. Eng. Sci.*, 21: 844-853, 1981.

- Henson, G. M., Cao, D., Bechtel, S. E., and Forest, M. G. A. Thin-filament melt spinning model with radial resolution of temperature and stress. *J. Rheol.*, 42: 329-360, 1998.
- Ottone, M. L., and Deiber, J. A. Modeling the Melt Spinning of Polyethylene Terephthalate. *Journal of Elastomers and Plastics*, 32:119-139, 2000.
- Ottone, M. L., and Deiber, J. A. A Numerical method for the viscoelastic melt spinning model with radial resolutions of temperature and stress field. *Industrial & Engineering Chemistry Research*, 41:6345-6353, 2002.
- Ottone, M. L., Peirotti, M. B., and Deiber, J. A. Computational spinning model to study different expressions proposed in the literature for the elongational viscosity evaluation from spinning experimental data. *Mecánica Computacional*. XXV: 21-40, 2006.
- Papanastasiou, T. C., Dimitriadis, V. D., Scriven, L. E., Macosko, C. W. and Sani, R. L. On the inlet stress condition and admissibility condition of fiber spinning. *Adv. Polym. Technol.*, 15: 237-244, 1996.
- Peirotti, M. B., Ottone, M. L., and Deiber, J. A., *Modeling melt spinning with stress induced crystallization at high take up velocities. 2-D numerical results for the PET melt*. S. R. Idelsohn and V. Sonzogni Eds. Applications of Computational mechanics in structures and fluids. Barcelona, 2005.
- Peirotti, M. B., Ottone, M. L., and Deiber, J. A. Numerical predictions of transient and steady rheometric functions of polyethylene melts through a spectral tensorial constitutive equation. *Mecánica Computacional*. XXV: 3-20, 2006.
- Peirotti, M. B., Deiber, J. A., Ressa, J. A., Villar, M. A., and Vallés, E. M. Relaxation modes of molten polydimethylsiloxane. *Rheologica Acta*, 37: 449-462, 1998.